Supporting Material

Electrochemical Potential-Driven Evolution of *CO Electronic Structure and Adsorption Configuration on Te-Based Diatomic Catalysts for Enhanced CO_2 Reduction

Yiming Yang, Xiaolong Li, Chengwei Yang, Guixian Ge* and Yanwen Zhang*

College of Sciences/State Key Laboratory of Advanced Energy Storage Materials and Technology, Shihezi University, Xinjiang, Shihezi, 832003, China.

* Corresponding authors.

E-mail addresses: geguixian@126.com (G. Ge), zyw_tea@shzu.edu.cn (Y. Zhang)

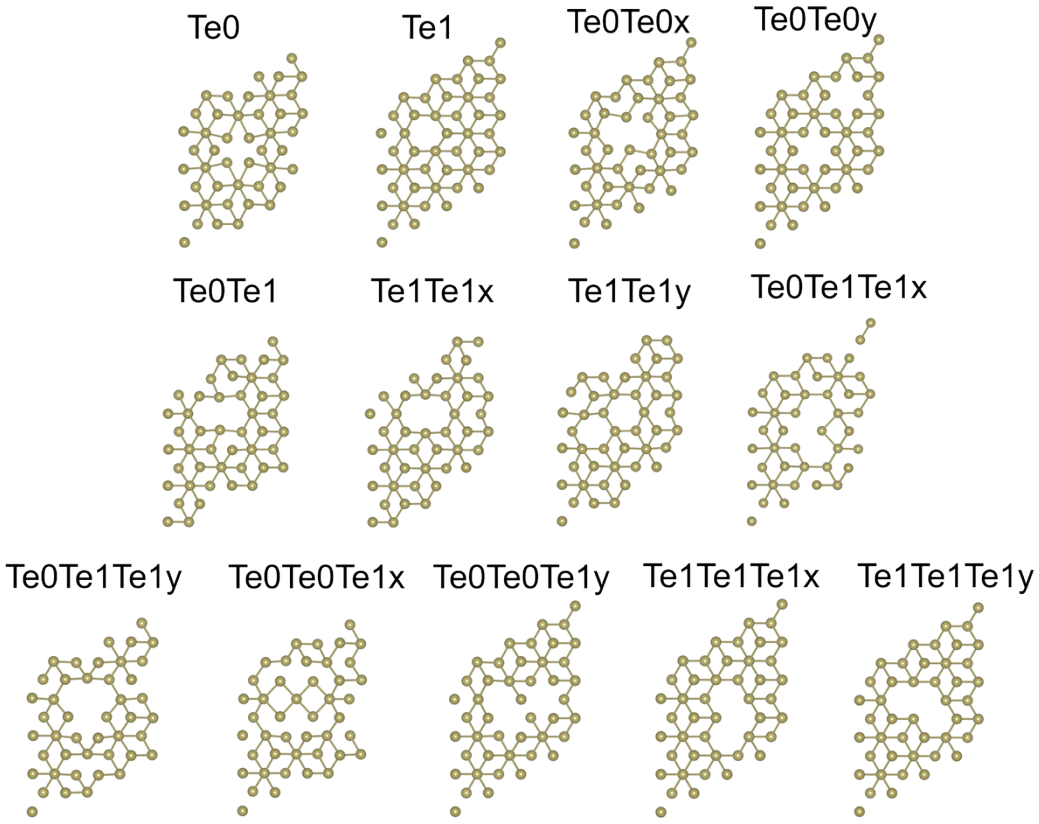

Figure S1 Thirteen representative point-defect configurations in a 4 × 4 × 1 unit cell.

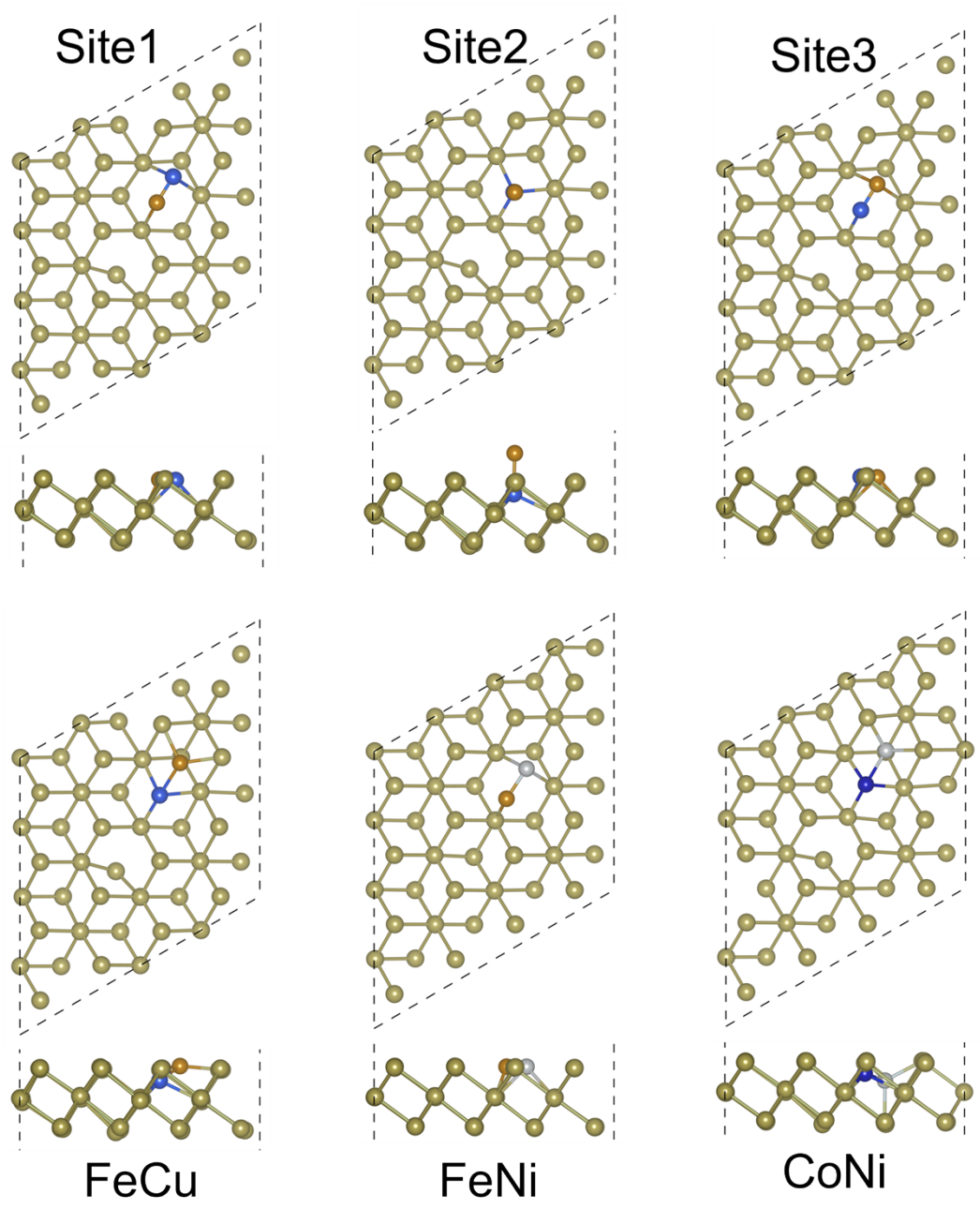

Figure S2 Three possible anchoring sites and the stable structures after optimization.

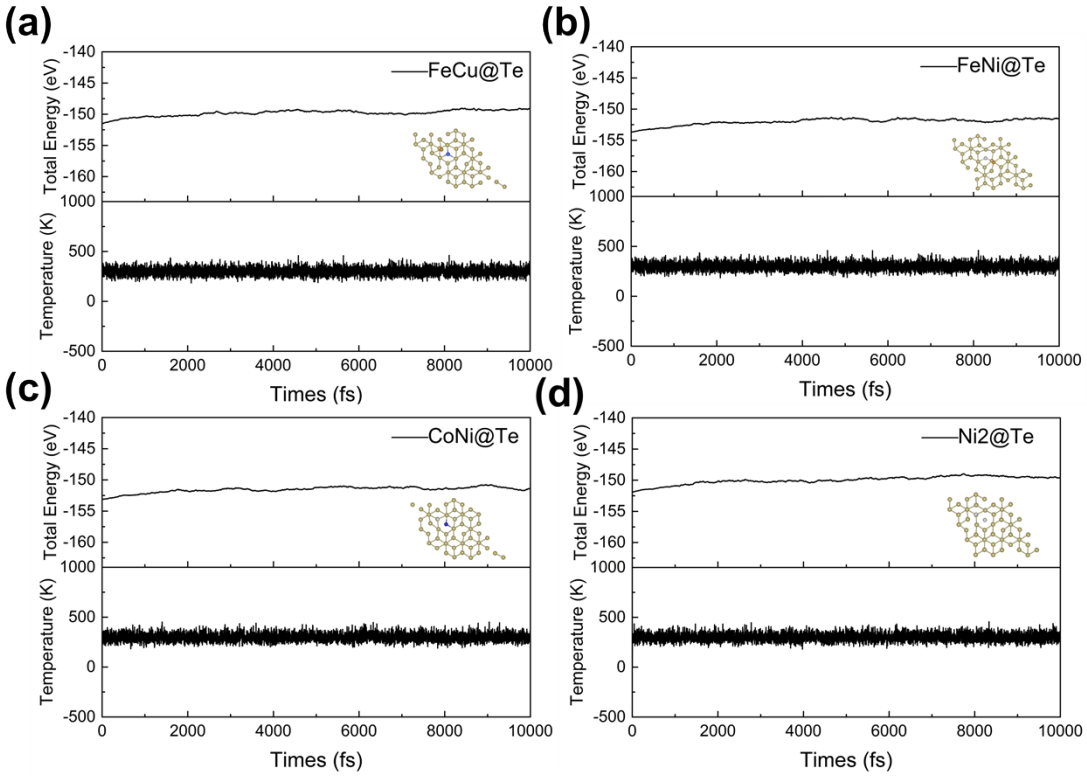

Figure S3 Taking FeCu, FeNi CoNi and Ni2 as examples, the AIMD simulation at 300K.

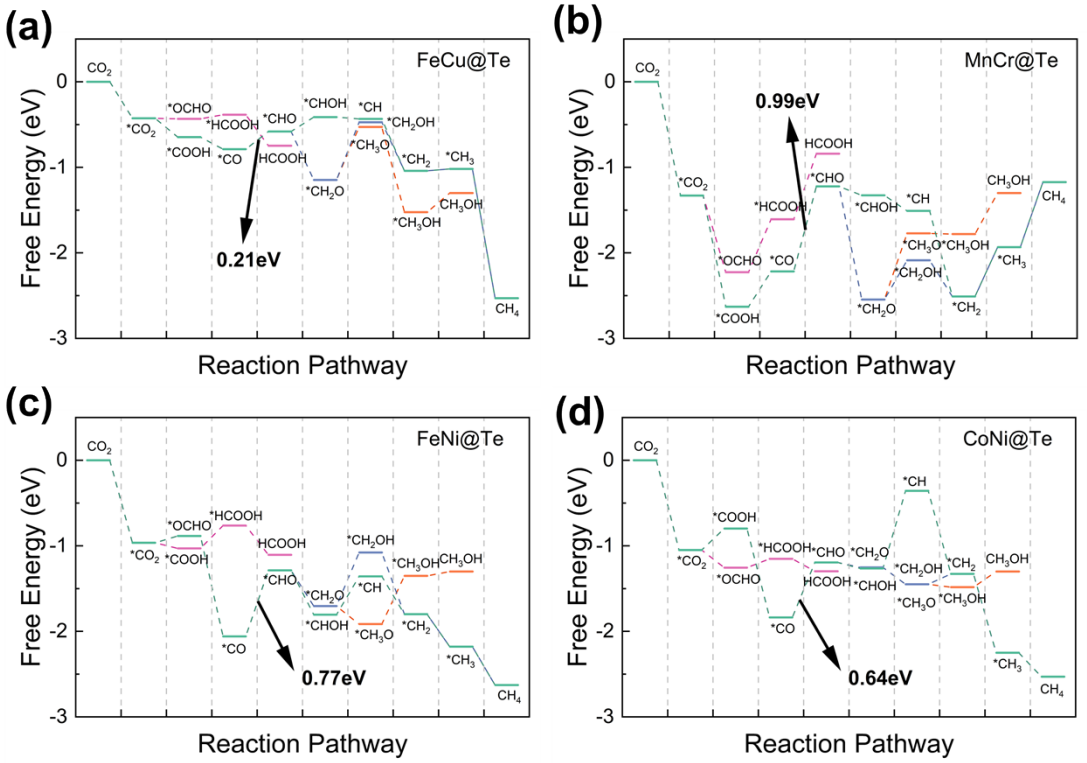

Figure S4 Calculated Gibbs free energies for MnCr@Te, CoNi@Te, FeNi@Te, and FeCu@Te.

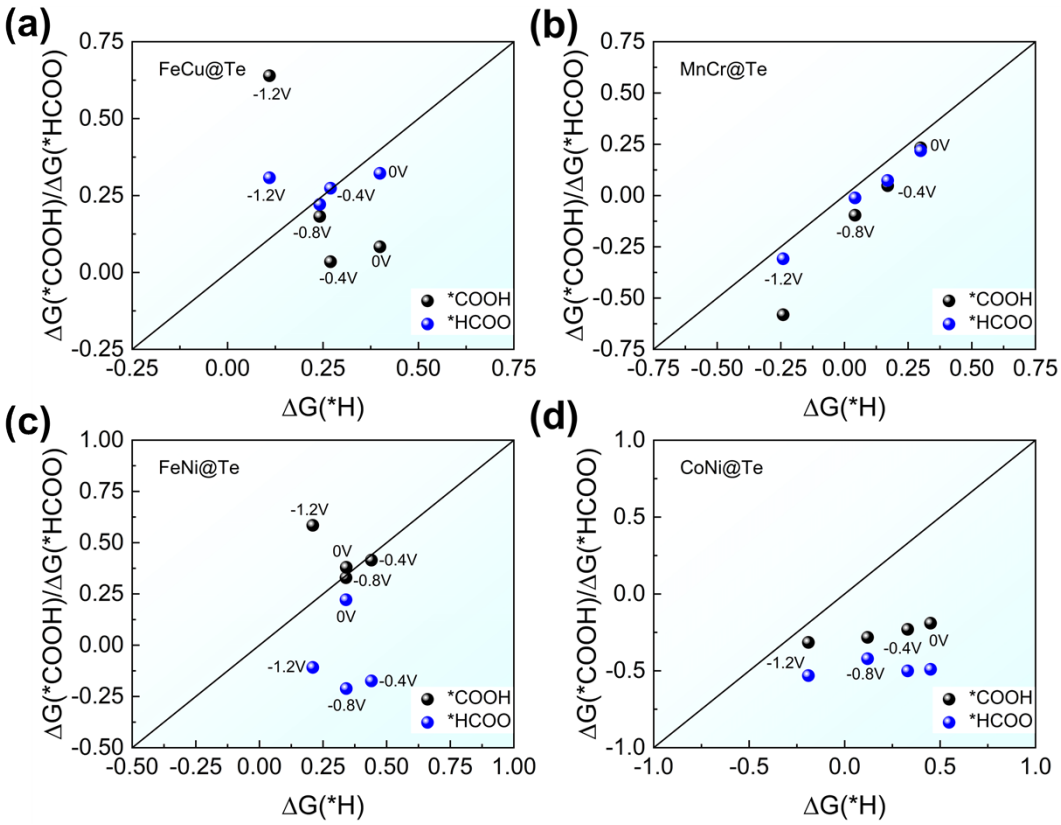

Figure S5 Comparative analysis of the calculated Gibbs free energy changes (ΔG) for the key intermediates *H, *COOH, and *HCOO under different applied potentials

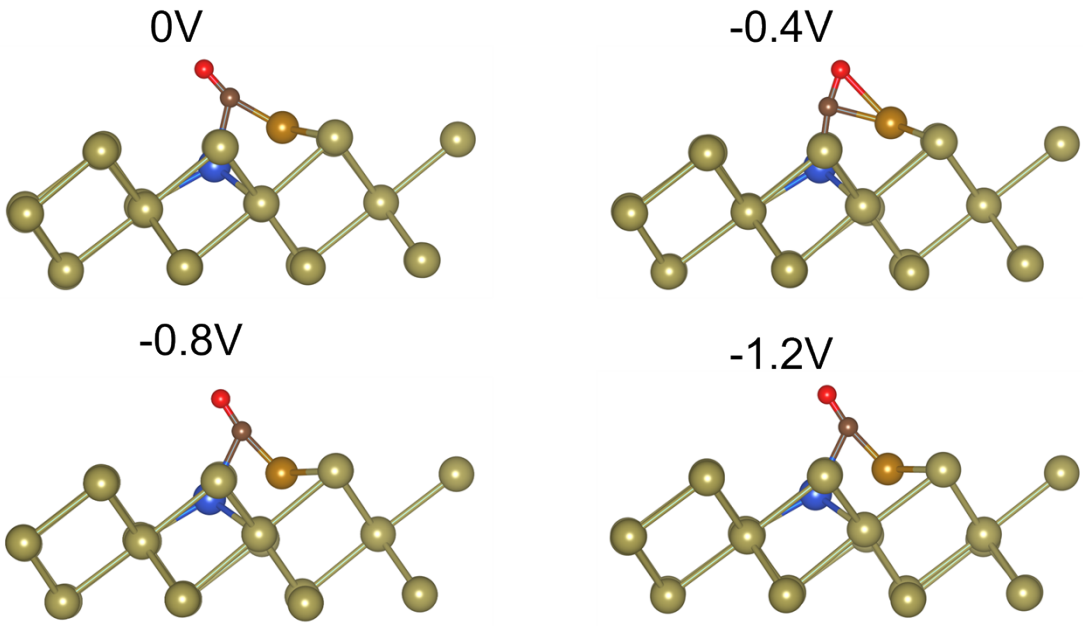

Figure S6 The structure of FeCu@Te adsorbing CO intermediates at different potentials

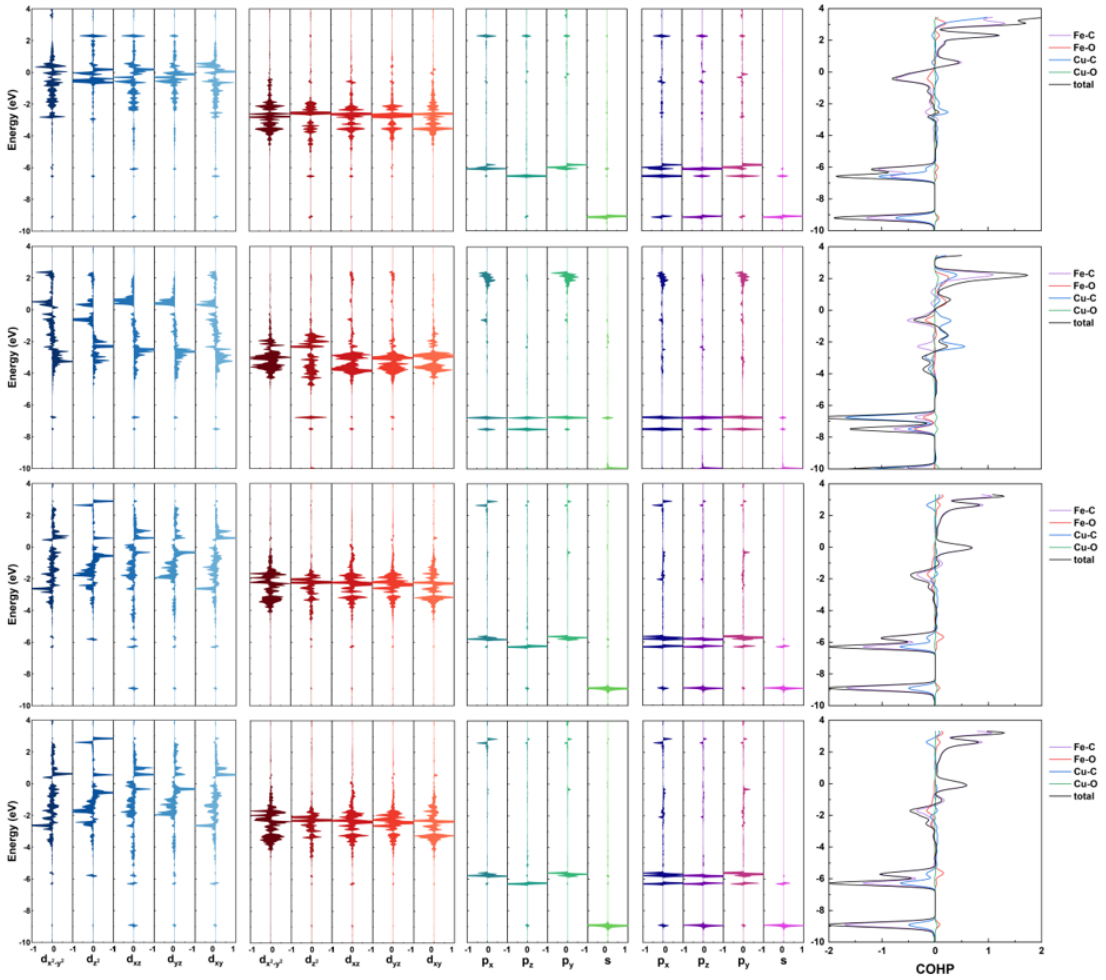

Figure S7 The PDOS and COHP of FeCu@Te adsorbing CO intermediates at different potentials

Table S1 Evaluation of the activation degree of the catalyst: adsorption free energy of CO_2, bond length, distance from the catalyst, bond angle, and charge transfer quantity.

Structures	G_{ads}(eV)	$L_{c\text{-}o}$(Å)	L(Å)	O-C-O(°)	$\Delta Q(CO_2)(\|e\|)$	$\Delta Q(O_1)(\|e\|)$
Te1	-0.195	1.175/1.177	4.083	179.92	0.059	0.059
Co2	-0.461	1.201/1.253	1.971	147.109	0.378	0.378
Fe2	-0.679	1.224/1.273	2.127	136.849	0.685	0.685
Ni2	-0.059	1.191/1.228	2.086	154.325	0.881	0.881
Co-Cr	-0.690	1.226/1.306	1.951	127.445	1.082	1.072
Co-Cu	0.409	1.238/1.241	1.999	140.794	1.072	1.033
Co-Mn	1.086	1.23/1.308	1.947	126.326	1.079	1.067
Co-Ni	-0.368	1.202/1.257	1.945	146.901	1.038	1.015
Cu-Cr	-0.395	1.224/1.286	2.065	133.1	1.054	1.069

Cu-Mn	-2.001	1.222/1.276	2.08	135.462	1.040	1.056
Fe-Co	-0.451	1.208/1.263	1.951	143.813	1.034	1.058
Fe-Cr	-0.492	1.24/1.08	1.981	131.309	1.053	1.083
Fe-Cu	0.254	1.26/1.231	2.005	139.759	1.033	1.051
Fe-Mn	-1.694	1.23/1.293	1.994	132.06	1.045	1.078
Fe-Ni	-0.284	1.259/1.246	1.938	137.616	1.032	1.032
Mn-Cr	-0.649	1.224/1.296	2.067	134.973	1.078	1.041
Ni-Cr	-0.639	1.213/1.279	1.98	133.616	1.054	1.079
Ni-Cu	0.421	1.213/1.26	2.016	138.704	1.043	1.052
Ni-Mn	-0.477	1.217/1.284	1.974	132.173	1.055	1.082

Table S2 The ICOHP between each atom of the FeCu@Te catalyst when adsorbing CO varies under different potentials.

ICOHP	0V	-0.4V	-0.8V	-1.2V
Fe-C	-1.552	-0.913	-2.228	-2.250
Fe-O	-0.128	-0.203	-0.188	-0.189
Cu-C	-0.585	-0.969	-0.441	-0.438
Cu-O	-0.029	-0.103	-0.024	-0.022

Table S3 Potential-determining step (PDS) and limiting potential (U_L) of the FeCu@Te catalyst under NCS and CPS conditions at different applied potentials.

State(NCS/CPS)	**potential-determining step (PDS)**	**U_L(V)**
NCS	*CO → *CHO	-0.21
CPS(0V)	*CO → *CHO	-0.58
CPS(-0.4V)	*CHOH → *CH	-0.26
CPS(-0.8V)	*CO → *CHO	-0.63
CPS(-1.2V)	*CO → *CHO	-0.67

Table S4 the ΔG values for steps 1–8 (*CO_2 → *COOH → *CO→ *CHO → *CH_2O → *CH_2OH → *CH_2→ *CH_3 → *CH_4)

State	**ΔG_1**	**ΔG_2**	**ΔG_3**	**ΔG_4**	**ΔG_5**	**ΔG_6**	**ΔG_7**	**ΔG_8**
CPS(0V)	0.083	-0.755	0.583	-0.073	0.140	-0.566	-0.252	-1.118

CPS(-0.4V)	0.035	-0.142	-0.174	0.016	0.266	-0.367	-0.426	-1.173
CPS(-0.8V)	0.182	-1.045	0.635	0.322	0.266	-0.617	-0.284	-1.337
CPS(-1.2V)	0.639	-1.092	0.678	0.385	-0.106	-0.267	-0.360	-1.249
NCS(0V)	-0.220	-0.141	0.207	0.168	-0.022	-0.606	0.022	-1.512
NCS(-0.4V)	-0.620	-0.541	-0.193	-0.232	-0.422	-1.006	-0.378	-1.912
NCS(-0.8V)	-1.020	-0.941	-0.593	-0.632	-0.822	-1.406	-0.778	-2.312
NCS(-1.2V)	-1.420	-1.341	-0.993	-1.032	-1.222	-1.806	-1.178	-2.712